

## Haptic Shared Control for Dissipating Phantom Traffic Jams

Koerten, Klaas O.; Abbink, David A.; Zgonnikov, Arkady

**DOI**

[10.1109/THMS.2023.3315519](https://doi.org/10.1109/THMS.2023.3315519)

**Publication date**

2024

**Document Version**

Final published version

**Published in**

IEEE Transactions on Human-Machine Systems

**Citation (APA)**

Koerten, K. O., Abbink, D. A., & Zgonnikov, A. (2024). Haptic Shared Control for Dissipating Phantom Traffic Jams. *IEEE Transactions on Human-Machine Systems*, 54(1), 11-20.  
<https://doi.org/10.1109/THMS.2023.3315519>

**Important note**

To cite this publication, please use the final published version (if applicable).  
Please check the document version above.

**Copyright**

Other than for strictly personal use, it is not permitted to download, forward or distribute the text or part of it, without the consent of the author(s) and/or copyright holder(s), unless the work is under an open content license such as Creative Commons.

**Takedown policy**

Please contact us and provide details if you believe this document breaches copyrights.  
We will remove access to the work immediately and investigate your claim.

***Green Open Access added to TU Delft Institutional Repository***

***'You share, we take care!' - Taverne project***

**<https://www.openaccess.nl/en/you-share-we-take-care>**

Otherwise as indicated in the copyright section: the publisher is the copyright holder of this work and the author uses the Dutch legislation to make this work public.

# Haptic Shared Control for Dissipating Phantom Traffic Jams

Klaas O. Koerten , David. A. Abbink , *Senior Member, IEEE*, and Arkady Zgonnikov , *Member, IEEE*

**Abstract**—Traffic jams occurring on highways cause increased travel time as well as increased fuel consumption and collisions. So-called *phantom traffic jams* are traffic jams that do not have a clear cause, such as a merging on-ramp or an accident. Phantom traffic jams make up 50% of all traffic jams and result from instabilities in the traffic flow that are caused by human driving behavior. Automating the longitudinal vehicle motion of only 5% of all cars in the flow can dissipate phantom traffic jams. However, driving automation introduces safety issues when human drivers need to take over the control from the automation. We investigated whether phantom traffic jams can be dissolved using haptic shared control. This keeps humans in the loop and thus bypasses the problem of humans' limited capacity to take over control, while benefiting from most advantages of automation. In an experiment with 24 participants in a driving simulator, we tested the effect of haptic shared control on the dynamics of traffic flow and compared it with manual control and full automation. We also investigated the effect of two control types on participants' behavior during simulated silent automation failures. Results show that haptic shared control can help dissipating phantom traffic jams better than fully manual control but worse than full automation. We also found that haptic shared control reduces the occurrence of unsafe situations caused by silent automation failures compared to full automation. Our results suggest that haptic shared control can dissipate phantom traffic jams while preventing safety risks associated with full automation.

**Index Terms**—Active pedals, driving simulator, haptic shared control, longitudinal vehicle motion, phantom traffic jams, silent automation failure.

## I. INTRODUCTION

**T**RAFFIC jams have far-reaching consequences, such as longer travel times, more frequent collisions, and increased fuel consumption and emissions due to the stop-and-go behavior of vehicles in traffic jams [1], [2]. In many cases, traffic jams can be traced to accidents, sharp curves, on-ramps, or sudden lane changes of vehicles. However, up to 50% of all traffic jams

do not have a distinct cause [3]; these are often called *phantom traffic jams*. Investigating possible ways to reduce the occurrence of phantom traffic jams can, therefore, help to curb enormous costs associated with traffic congestion.

Vehicle density plays a crucial role in the formation of phantom traffic jams. Each road has a certain critical density for each velocity. If car density increases beyond this density, the flow becomes unstable, and the average speed of the vehicles drops below the speed limit [4]. However, even though high density is a prerequisite for the formation of phantom traffic jams [5], it has been argued that stochastic velocity fluctuations inherent in the behavior of human drivers are what triggers them [6], [7]. While in sparse traffic these fluctuations do not have a major impact on the traffic flow, when the density becomes high enough, these fluctuations can propagate and amplify, thereby causing a phantom traffic jam [8]. Sugiyama et al. [9] and Tadaki et al. [10] have shown this phenomenon occurring on a single-lane ring road with no external causes. Initially, drivers manage to keep a constant speed, but after some time, oscillations start to happen, the flow eventually becomes unstable, and stop-and-go waves start to form. Furthermore, commercially available adaptive cruise control systems can amplify disturbances of traffic flow just as much as human drivers on their own do [11]. Overall, the reviewed studies show that natural human driving behavior, as well as driving automation, can lead to the occurrence and preservation of phantom traffic jams.

Existing approaches to the problem of phantom traffic jams can be divided into two categories. *Centralized solutions* use sensors in the infrastructure to identify phantom traffic jams and solve them using dynamic traffic signs to open up additional traffic lanes or change the speed limit. These solutions have been shown to stabilize dense traffic [12], but require substantial adaptations to existing infrastructure; in addition, dynamic speed limits might slow down traffic when this is unnecessary, because there is a delay between the time when the traffic jam has been solved and when the system has noticed this and adapted the speed limit. *Decentralized solutions* use automated vehicles as agents to stabilize traffic locally to dissipate phantom traffic jams. One type of decentralized solution lets multiple automated vehicles drive behind one another in a platoon [13]. Another type stabilizes traffic flow with a small number of automated vehicles (typically no more than 10%) equipped with cruise control specifically developed for this [14], [15], [16]. Automation-based solutions only require small adaptations to vehicles and can work for realistic penetration rates of cars equipped with adaptive cruise control.

Manuscript received 28 November 2022; revised 2 May 2023 and 21 July 2023; accepted 19 August 2023. Date of publication 10 January 2024; date of current version 26 January 2024. This article was recommended by Associate Editor J. YC Chen.

This work involved human subjects in its research. Approval of all ethical and experimental procedures and protocols was granted by Human Research Ethics Committee of the Delft University of Technology.

The authors are with the Department of Cognitive Robotics, Faculty of Mechanical, Maritime and Materials Engineering, Delft University of Technology, 2628 CD Delft, The Netherlands (e-mail: k.koerten@hotelschool.nl; d.a.abbink@tudelft.nl; a.zgonnikov@tudelft.nl).

The data and the code accompanying this article are available at <https://osf.io/rpwx/>.

Color versions of one or more figures in this article are available at <https://doi.org/10.1109/THMS.2023.3315519>.

Digital Object Identifier 10.1109/THMS.2023.3315519

However, automating vehicles comes at a cost. When the longitudinal motion of a car is fully automated, the drivers function as supervisors instead of operators, i.e., the human is taken out of the loop [17]. According to [18], when humans become supervisors, their skills as operators of the task decline over time. However, they still remain responsible for taking over the task when things get too complicated for the automation. Typical problems associated with automation are the vigilance decrement [19], where the drivers' attention declines over time, and overreliance, where the drivers put too much trust in the automation and do not take over when necessary [17]. Other disadvantages are increased reaction times and decreased performance when the human needs to take over. Human drivers sometimes do need to take over, because adaptive cruise control systems may experience difficulty in tracking a leading vehicle [20] or in identifying an approaching stationary queue [21]. However, Rudin-Brown and Parker [22] show that reaction times of drivers increase when they rely on adaptive cruise control. Together, these effects could result in unsafe driving situations, especially in the dense traffic situations in which phantom traffic jams occur. This represents a potential pitfall of traffic stabilization solutions based on full automation of longitudinal vehicle control [23].

As long as driving automation is not perfect, human drivers need to be able to take over control at any time. This requires them to stay engaged in the driving task, but how can they avoid losing vigilance while performing the daunting task of supervising automation? Continuously sharing the control between the human operator and the automation ensures driver engagement while still benefiting from the advantages of automation. In a simulator study, Jiang et al. [24] showed how a sharing algorithm dampens traffic waves on a circular ring road. This shared controller takes as input the average of the human driver's pedal positions and the ideal positions. This means that a car equipped with this shared controller is half automated, which could still result in safety issues. Imagine, for example, the case where a human wants to press the brake pedal suddenly, but the automation does not; then, the human driver can only brake half as hard because the automation does not want to press the brake. This could cause the car to not slow down fast enough to prevent an accident.

*Haptic* shared control, on the other hand, does allow for full human intervention by making both the human operator and the automation exert forces on the accelerator and brake pedal. The position of the pedals determines the acceleration or deceleration of the car [25]. Haptic shared control for lateral vehicle motion can significantly improve safety compared to full automation when a silent automation failure happens [26]. Previous research has reported improved performance with haptic feedback on the accelerator pedal for car-following [27], for making drivers more compliant to speed limits [28] and for promoting a more eco-friendly driving style [29], [30].

These results suggest that haptic shared control could potentially be an efficient solution to managing phantom traffic jams in a decentralized way while avoiding the pitfalls of automation. However, the effect of haptic shared control on traffic jams has not yet been investigated. This research aims to address this gap in the literature. The main contribution of this article is an

experimental evaluation of the efficacy of haptic shared control for dissipating phantom traffic jams jointly with the robustness of human drivers' reaction to silent automation failures. We propose a novel haptic shared gas pedal controller that incorporates the algorithm for dissipating phantom traffic jams from [15]. This algorithm was chosen because it has been tested in a real life driving experiment on a ring road and has shown significant damping of phantom traffic jams for realistic penetration rates. We then test its performance in a driving simulator experiment with 24 participants. As benchmarks, we use the manual and fully automated conditions.

## II. HAPTIC SHARED CONTROLLER DESIGN

The proposed haptic shared controller includes software and hardware components. The software part calculates the haptic forces that the controller applies to the pedals. The hardware includes a physical interface through which a human operator interacts with the automation.

### A. Software Design

To implement haptic shared control, we first calculate the target longitudinal speed for the tested scenario using the algorithm proposed by Stern et al. [15]. We calculate the target speed in the following way:

$$v^{\text{cmd}} = \begin{cases} 0, & \text{if } \Delta x \leq \Delta x_1 \\ v \frac{\Delta x - \Delta x_1}{\Delta x_2 - \Delta x_1}, & \text{if } \Delta x_1 < \Delta x \leq \Delta x_2 \\ v + (U - v) \frac{\Delta x - \Delta x_2}{\Delta x_3 - \Delta x_2}, & \text{if } \Delta x_2 < \Delta x \leq \Delta x_3 \\ U, & \text{if } \Delta x_3 < \Delta x \end{cases} \quad (1)$$

where

$$\Delta x_k = \Delta x_k^0 + \frac{1}{2d_k} (\Delta v_-)^2, \quad \text{for } k = 1, 2, 3. \quad (2)$$

In these equations,  $v^{\text{cmd}}$  is the target speed,  $U$  is the maximum speed on the road,  $\Delta x$  is the bumper-to-bumper gap between the ego and leading vehicles,  $v$  is the current speed, and  $\Delta v_-$  is the difference in longitudinal velocity between the ego and leading vehicles.  $\Delta x_k^0$  and  $d_k$  are constant parameters, directly taken from [15]:  $\Delta x_1^0 = 4.5$  m,  $\Delta x_2^0 = 5.25$  m,  $\Delta x_3^0 = 6.0$  m,  $d_1 = 1.5$  m/s<sup>2</sup>,  $d_2 = 1$  m/s<sup>2</sup>, and  $d_3 = 0.5$  m/s<sup>2</sup>.

As (1) shows, the target speed is determined based on the gap to the leading vehicle,  $\Delta x$ . Different thresholds for this gap,  $\Delta x_k$ , are defined as a combination of the base distance gap,  $\Delta x_k^0$ , and a term based on the velocity difference between the two vehicles,  $\Delta v_-$ . Stern et al. [15] provide a more detailed description of this algorithm.

The difference between  $v^{\text{cmd}}$  and  $v$  is the input for the pedal controller. This controller does the following:

$$\begin{aligned} \text{if } v^{\text{cmd}} - v > 0 & \Rightarrow \text{accelerate} \\ \text{if } 0 \geq v^{\text{cmd}} - v \geq -0.25 & \Rightarrow \text{do nothing} \\ \text{if } v^{\text{cmd}} - v < -0.25 & \Rightarrow \text{brake.} \end{aligned} \quad (3)$$

Equation (3) shows that the control actions are to: 1) do nothing, making the car brake on the engine, where both pedals

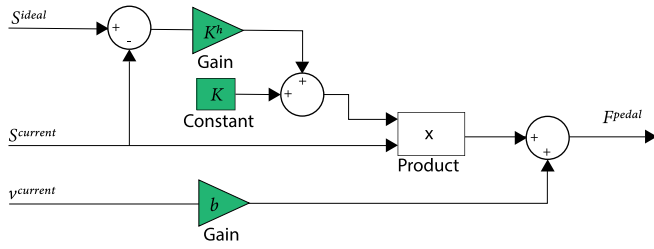


Fig. 1. Block diagram of the accelerator pedal for the haptic shared control case.

get released; 2) press the accelerator pedal and release the brake pedal to accelerate; or 3) press the brake pedal and release the accelerator pedal to decelerate. When acceleration or deceleration needs to happen, the pedal position of the accelerator or the brake pedal is determined by feeding the difference in speed into the accelerator or decelerator controller, respectively. Both controllers are proportional–integral–derivative (PID) controllers that produce the target pedal positions,  $S_{\text{acc}}^{\text{target}}$  and  $S_{\text{brake}}^{\text{target}}$ . The gains of the accelerator controller are  $K_p = 1$ ,  $K_i = 0.01$ , and  $K_d = 0.05$  and the gains of the decelerator controller are  $K_p = 0.7$ ,  $K_i = -0.04$ , and  $K_d = 0.1$ . The controllers were tuned by running the ring road simulation and feeding the outputted target pedal position as the current position into the simulated ego vehicle. The gains were then adjusted until wave dampening behavior similar to [15] was achieved.

The haptic accelerator and brake pedals that we used are connected to control loaders, which simulate the forces and movements that actual pedals would exert on the driver’s foot [31]. Software controls the virtual mass, damping, stiffness, and the forces that the pedals exert on the driver’s foot. The default behavior of both pedals is spring-damper behavior.

For the haptic shared controller, we use the difference between the current pedal position  $S^{\text{current}}$  and the target position  $S^{\text{target}}$  to set the stiffness  $K$  of the accelerator pedal to  $K^{hc}$  (see Fig. 1)

$$K^{hc} = K + K^h \times (S^p - S^{\text{target}}). \quad (4)$$

The choice to use stiffness feedback was made. This is done because when the pedal moves from the targeted position, it gets pushed back with a virtual spring that increases its force depending on the distance from the targeted position. This is less drastic than, for example, force feedback, that applies a sudden force when the pedal leaves the targeted position [32]. We initially provided feedback on both the accelerator and the brake pedal. However, in pilot studies, participants reported that haptic feedback on the brake pedal did not make them feel safe in the car. This was because a braking action is done to quickly slow down the car. When the driver would want to press the brake sooner or later than the automation, the brake would be less stiff or stiffer than expected. This would result in unwanted behavior of the brake pedal and, therefore, in an unwanted braking action, making the driver feel unsafe.

For these reasons, we made the choice to only provide haptic feedback on the accelerator pedal. The stiffness feedback was set in such a way that participants would notice the increased stiffness as well as the decreased stiffness. The stiffness gains for which this was the case were  $300 \text{ N/rad}^2$  for the increase

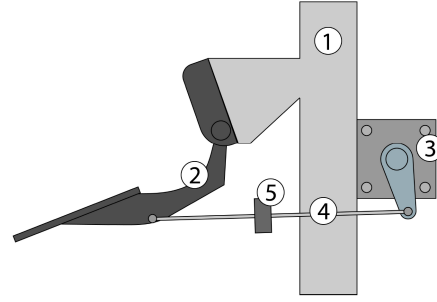


Fig. 2. Setup of the active accelerator pedal. On the frame (1), the pedal (2) is adjusted with the control loader (3), which is connected to the pedal via a rod (4) with a force cell (5) on it.



Fig. 3. Fixed-base driving simulator setup.

and  $-30 \text{ N/rad}^2$  for the decrease. Because the driver has its foot pressing on the pedal, increased stiffness needed to be higher for the driver to feel the feedback.

## B. Hardware Design

Fig. 2 shows a picture of the active pedals, which are made from Audi pedals. The pedals are connected to a servo motor via a metal rod, with an axial force sensor placed in the middle of it. This setup is called a control loading system. A feedback loop, closed with the axial force sensor, controls the force that the servo motor applies to the linkage. The pedal has the spring-damper behavior, meaning that the pedal force is calculated as follows:

$$F^{\text{pedal}} = K \times S^p + v^p \times b \quad (5)$$

where  $K$ ,  $S^p$ ,  $v^p$ , and  $b$  are the pedal stiffness, pedal position, pedal speed, and pedal damping, respectively. The active pedal setup was installed in a custom-built fixed-base simulator (see Fig. 3). The simulator consists of a car seat and a frame carrying the pedals, a steering wheel, a 55-in monitor, speakers, and a set of computers on which the simulation runs. We used the IPG CarMaker software suite, which was integrated with the commercially available Cruden Panthera software [33]. This software setup combines the steering wheel and pedal control inputs, the audiovisual rendering, and the simulated scenario into one coherent real-time simulation.

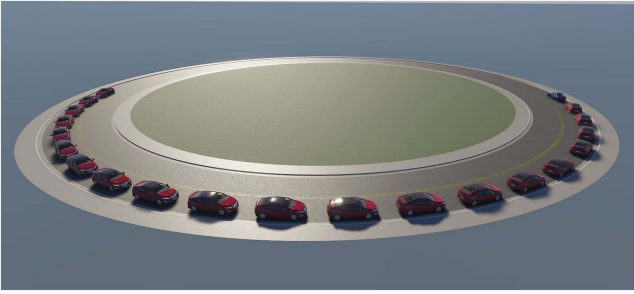


Fig. 4. Bird's-eye view of the simulated ring road environment. The blue car is the ego vehicle and the red cars are the simulated traffic cars.

### III. EXPERIMENT SETUP

#### A. Scenario

We evaluated the haptic shared controller in a ring road scenario with a radius of 42 m and 21 cars on it, including the ego vehicle (see Fig. 4). This scenario is based on earlier studies that observe traffic jam formation on ring roads [9], [10], [15]. We took the circumference and number of cars in our scenario from [15] because the  $\Delta x_k^0$  and  $d_k$  parameters from (1) are tuned specifically for this scenario. After pilot studies, we decided not to let the cars in the simulation start equally spaced around the ring road as in [9], [10], and [15], but to concentrate them behind the ego vehicle at the start of the experiments. Because of this, there was an initial traffic jam that the ego vehicle drives into after finishing the first lap, allowing the traffic jam dissipation of the different means of control to be evaluated without waiting for the formation of a traffic jam. The 20 traffic cars are controlled by the IIDMACC driver model [4], with some minor adjustments provided by IPG CarMaker [34].

#### B. Participants

Twenty-four participants were recruited. The average age was 32.6 years (standard deviation = 12.0). They had held a drivers' license for 13.2 years on average (standard deviation = 10.9) and drove 4.2 h per week on average (standard deviation = 4.4).

#### C. Experimental Conditions

The experiments consisted of three driving sessions of 8 min, during which we asked participants to drive on the simulated ring road. During each session, we evaluated participants' behavior in one of the following three conditions.

- 1) *Manual control*: In this condition, the participant fully controls the accelerator and the brake pedal.
- 2) *Haptic shared control*: In this condition, the participants' control input was combined with the input of the controller proposed by Stern et al. [15] in the way described in Section II.
- 3) *Fully automated control*: In this condition, the accelerator and the brake pedal are completely controlled by the input controller from Stern et al. [15]. The participant controls the steering wheel and monitors the car. The participant is able to intervene by stepping on the pedals.

Participants were instructed to drive like they would normally do on a highway and in a traffic jam. Before the start of the measurements, participants drove in the manual condition for 2 min to get used to the controls and the simulator. The order in which the conditions were tested was randomized across participants to counterbalance potential learning effects. During the manual and haptic condition, participants were instructed to control the steering wheel and the pedals themselves. In the automated condition, they were instructed only to steer and watch the road, as both pedals were fully automated. In this condition, participants were instructed to only interfere with the pedals when a situation was deemed unsafe.

#### D. Silent Automation Failure

In the haptic and fully automated conditions, a silent automation failure occurred after 8 min of driving. It simulated a real-life situation in which the camera system fails to detect the leading vehicle. We simulated this by sending a value of 1000 m for the bumper-to-bumper gap to the velocity controller, resulting in a  $v^{\text{cmd}}$  equal to  $U$ , causing the haptic accelerator pedal to decrease its stiffness and the automated pedal to get depressed until  $U$  was reached. When this happened, the participant needed to intervene to prevent collision with the leading vehicle. After the participant regained control of the ego vehicle, we terminated the driving session.

#### E. Hypotheses

We hypothesized that, compared to manual control, the haptic shared controller would reduce the motion variability of the individual vehicle and the traffic flow as a whole and reduce the traffic jam lifetime and the number of times the traffic jam is not dissipated. We also hypothesized that the haptic shared controller will result in higher throughput, compared to the manual driving condition. At the same time, we hypothesized that the fully automated controller will improve these metrics even further compared to the haptic shared controller. Finally, we hypothesized that the haptic shared controller will be safer than the fully automated controller in the event of silent automation failure, resulting in larger minimal gap after the failure and reduced number of collisions.

#### F. Statistical Analyses

To compare the three different means of control, for each participant, we calculated metrics from the signals recorded during each session. These metrics quantified different aspects of the ego vehicle motion and the behavior of the entire vehicle platoon. To evaluate differences between the metrics that represent continuous variables, we performed paired  $t$ -tests ( $df = 23$ ). To compare discrete-valued metrics representing the occurrence of an event, we performed the McNemar test [35]. For the  $t$ -test as well as the McNemar test, we deem the difference in metric values to be significant when the  $p$ -value is lower than 0.05.

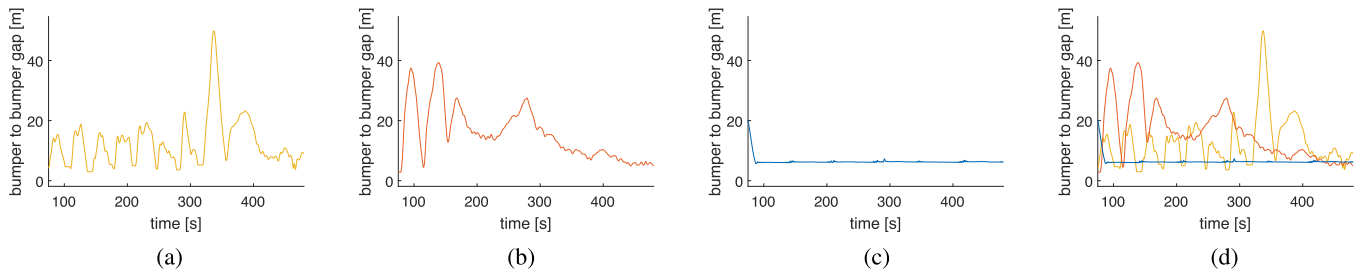


Fig. 5. Bumper-to-bumper gap between the ego vehicle and the leading vehicle over time for a representative participant for each condition. (a) Manual. (b) Haptic. (c) Automatic. (d) Combined.

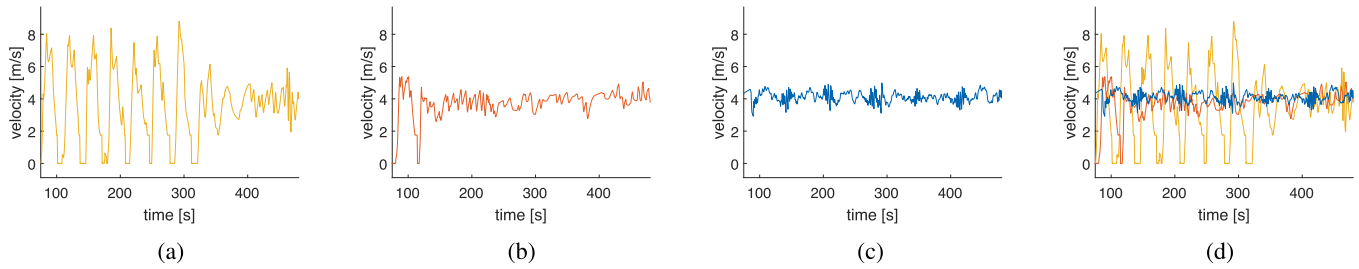


Fig. 6. Velocity of the ego vehicle over time for a representative participant for each condition. (a) Manual. (b) Haptic. (c) Automated. (d) Combined.

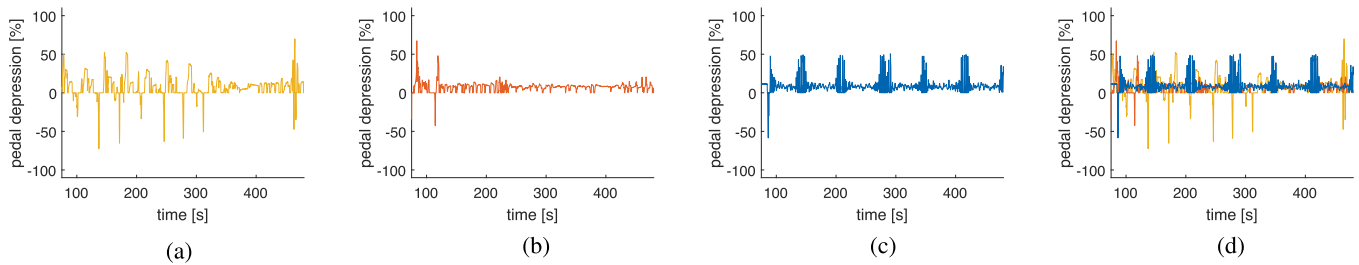


Fig. 7. Pedal depression of the ego vehicle over time for a representative participant for each condition. Positive values correspond to accelerator pedal depression; negative values correspond to brake pedal depression. (a) Manual. (b) Haptic. (c) Automated. (d) Combined.

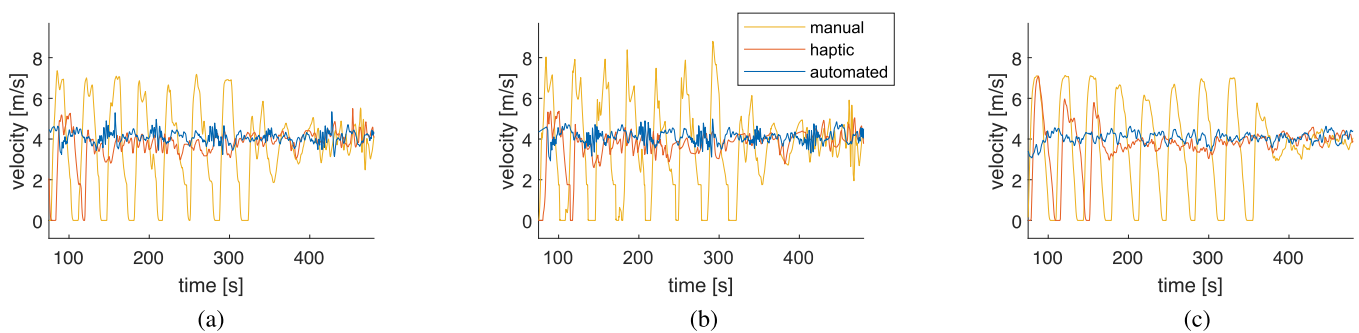


Fig. 8. Velocity of the following, ego, and leading vehicles for a representative participant for each condition. (a) Following. (b) Ego. (c) Leading.

## IV. EVALUATION RESULTS

### A. Typical Participant Behavior

Figs. 5–8 illustrate the behavior of a representative participant in the three conditions, starting after the transient period of 75 s.<sup>1</sup>

<sup>1</sup>Figures illustrating the behavior of all other participants can be found in the online supplementary material (<https://osf.io/rpwx>).

The dynamics of the gap between the ego vehicle and the leading vehicle (see Fig. 5) shows that in the manual and haptic cases, the driver is free to determine this gap, while in the automated case, the algorithm keeps the gap at a constant value of 6.5 m.

Velocity traces (see Fig. 6) further highlight qualitative differences between the three conditions. In the manual case [see Fig. 6(a)], velocity initially oscillates between standstill (0 m/s) and the speed limit (7 m/s). After approximately 320 s,

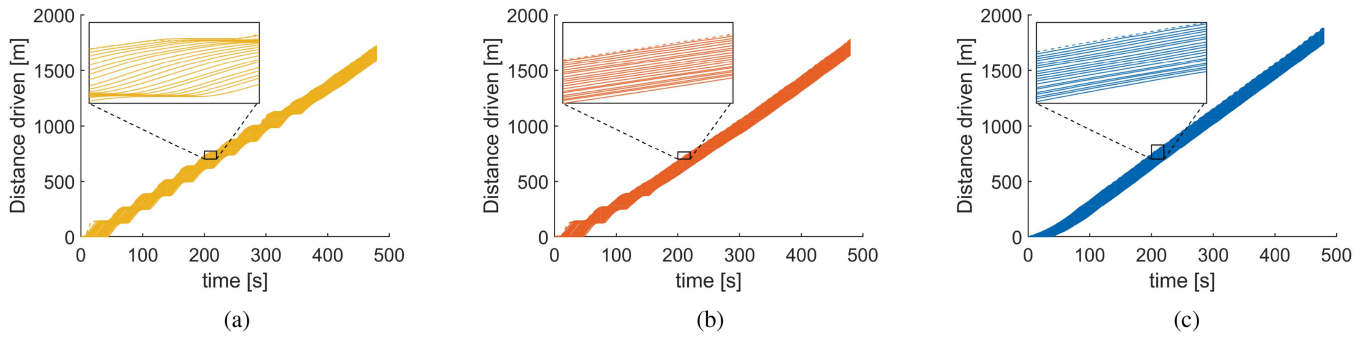


Fig. 9. Trajectories of all vehicles in the platoon. (a) Manual. (b) Haptic. (c) Automated.

the stop-and-go wave is dissipated and the car drives at a velocity that oscillates around 4 m/s. The haptic shared control condition [see Fig. 6(b)] shows similar oscillatory behavior at the start of the experiment, but this already stops after 120 s. Finally, the automatic condition [see Fig. 6(c)] shows a velocity signal that oscillates around 4 m/s during the entire experiment, meaning that the traffic jam that is present at the start of the experiment is dissipated in less than 75 s.

The input signals of the ego vehicle (see Fig. 7) illustrate that (at least for this participant) the number of braking instances is reduced in the haptic shared control and fully automated conditions compared with the manual control condition. Interestingly, it also shows that the accelerator pedal positions for both the manual case and the automatic case are more extreme than those of the haptic case. For the manual and automatic cases, the pedal depression often reaches 50%, even after the traffic jam has already been dissipated.

To illustrate how the behavior of the ego vehicle influences the behavior of the neighboring vehicles, we plotted their velocities next to each other (see Fig. 8). The velocity profiles of the following [see Fig. 8(a)] and leading [see Fig. 8(c)] vehicles are similar to those of the ego vehicle, while their driving algorithms remain the same over the different conditions.

Finally, the trajectories of all vehicles in the platoon illustrate the dynamics of the phantom traffic jam (see Fig. 9).

### B. Ego Vehicle Motion Variability

We analyzed the variability of the ego vehicle motion in the three conditions, as quantified by the standard deviation of the ego vehicle velocity and the number of braking instances over each session.

On average, the standard deviation of the ego vehicle speed was significantly smaller in the haptic shared control condition compared to the manual control condition ( $t = 2.2028$ ,  $p = 0.0379$ ; see Fig. 10). The fully automated condition showed a further decrease ( $t = 4.8916$ ,  $p = 0.0001$  and  $t = 3.3727$ ,  $p = 0.0026$  when compared with the manual and haptic cases, respectively).

The number of braking instances of the ego vehicle in the haptic and automated conditions was significantly smaller than in the manual condition ( $t = -2.7550$ ,  $p = 0.0112$ , and

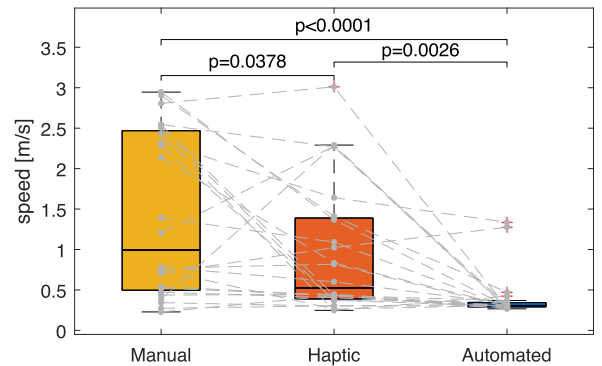


Fig. 10. Standard deviation of the speed of the ego vehicle for the three different conditions.

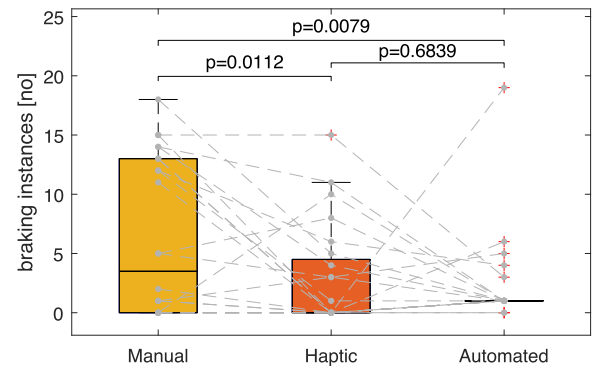


Fig. 11. Number of braking instances of the ego vehicle for each condition.

$t = -2.9061$ ,  $p = 0.0079$ , respectively; see also Fig. 11). However, there was no evidence that full automation reduces the number of braking instances compared to haptic shared control ( $t = 0.4123$ ,  $p = 0.6839$ ).

### C. Platoon Motion Variability and Traffic Jam Dissipation

Motion variability of all the vehicles in the platoon was quantified by the average standard deviation of the velocity across all vehicles. Higher values of this metric would indicate larger velocity fluctuations across the platoon.

Haptic shared control reduced the standard deviation of the speed for the entire platoon significantly compared to the manual condition ( $t = 2.1128$ ,  $p = 0.0456$ ; see Fig. 12). Automation



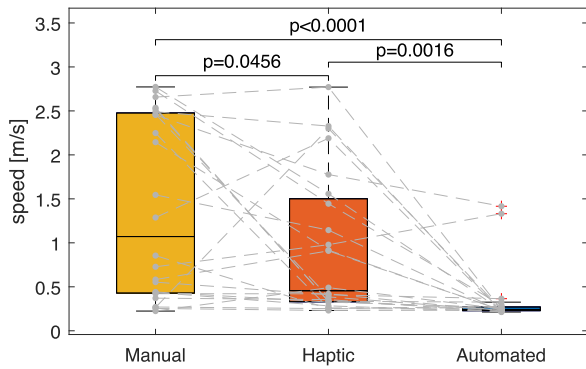


Fig. 12. Standard deviation of the speed of the vehicles for the three different conditions.

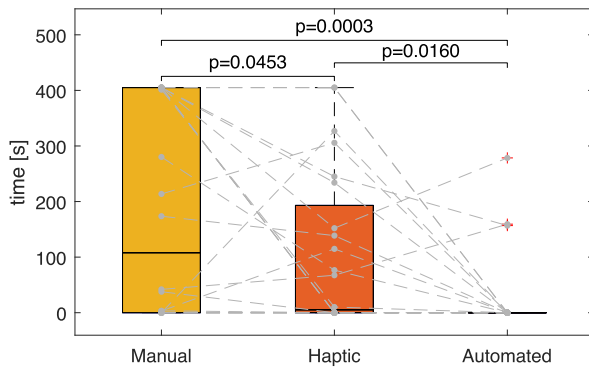


Fig. 13. Lifetime of the initially imposed traffic jam for the three conditions.

reduced it even further compared to both the haptic shared control as well as the manual case ( $t = 3.5731, p = 0.0016$  and  $t = 4.9012, p < 0.0001$ , respectively).

Efficiency of the traffic jam dissipation was measured by traffic jam lifetime and the road throughput. We defined the lifetime of the traffic jam as the first moment (after the transient period of 75 s) at which none of the cars had zero speed anymore. For the start time of the traffic jam, we took 75 s, as that was the moment the last vehicle took off. From this moment on, all the cars move and the initially imposed traffic jam is dissipated. If by the end of the session (480 s) the traffic jam was not dissolved, we considered its lifetime to be 405 s.

Lifetime of the initial traffic jam was lower in the haptic case compared to the manual case ( $t = 2.116, p = 0.0453$ ; see Fig. 13). In the automated case, the traffic jam lifetime was lower than in the manual case and the haptic shared control case ( $t = 4.1849, p = 0.0003$  and  $t = 2.5985, p = 0.0160$ , respectively). These comparisons, however, are subject to the ceiling effect due to the limited duration of the experiment. To provide further insight into differences between conditions, we analyzed the number of participants, which did not dissipate traffic jam by the end of the trial. In the manual control condition, 9 out of 24 participants did not manage to dissipate the traffic jam. In the haptic shared control case, it was not dissipated only by 2 out of 24 participants. In the automatic case, the jam was always dissipated. The differences between conditions are statistically significant when comparing haptic shared control to manual control (McNemar  $\chi^2 = 5.143, p = 0.02334$ ) and full automation with

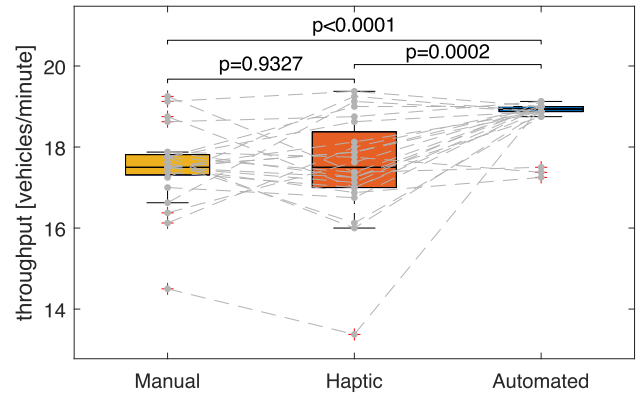


Fig. 14. Throughput of vehicles during the three different conditions.

manual control (McNemar  $\chi^2 = 7.111, p = 0.007661$ ). There is no evidence of a significant difference when comparing haptic shared control with automation (McNemar  $\chi^2 = 0.5, p = 0.4795$ ).

We calculated road throughput by counting the number of cars that have passed a virtual checkpoint on the ring road during the driving session. This number was divided by 8 to obtain the average number of vehicles that drive past the checkpoint of the road per minute.

The road throughput for the manual and haptic shared control case were in the same range, both in terms of median and variance (see Fig. 14). There was no evidence of a difference between these conditions ( $t = 0.0853, p = 0.9327$ ). The throughput for the fully automated condition, however, was higher than for the manual and haptic conditions ( $t = 4.3711, p = 0.0002$  and  $t = 4.8840, p < 0.0001$ , respectively).

#### D. Safety

Our setup including a silent automation failure occurring at the end of each trial allowed us to investigate how it was handled by the participants in each condition. Safety during the automation failure was measured based on the bumper-to-bumper gap between the ego vehicle and the leading vehicle (only for the haptic and the automated condition). We used the minimal bumper-to-bumper gap after the silent automation failure as a metric, as well as the occurrence of a collision (which was detected if the gap value reached 0).

In the fully automated condition, the simulated failure in the leading vehicle tracking meant that the automation depressed the accelerator pedal. This led to a decreasing bumper-to-bumper gap between the leading vehicle and the ego vehicle right after the failure (see Fig. 15). To avoid a collision, the driver needed to intervene and press the brake, after which the gap increased again. In 5 out of 24 participants, this automation failure caused a collision. Out of these five participants, four saw the automatic condition before the haptic condition.

For the haptic controller, the failure led to the accelerator pedal decreasing its stiffness. However, the pedal did not depress itself and because the drivers already had their foot on the pedal while driving, they only needed to reduce the pressure applied to the pedal to have the car slow down. In some of the cases,

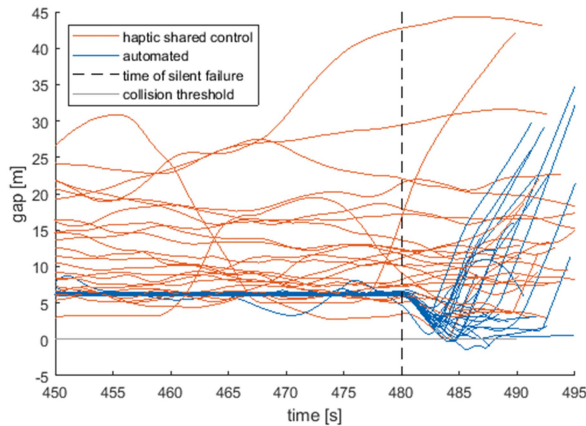


Fig. 15. Bumper-to-bumper gap between the ego vehicle and the leading vehicle from 450 s until the end of the run for the haptic shared control and automated conditions.

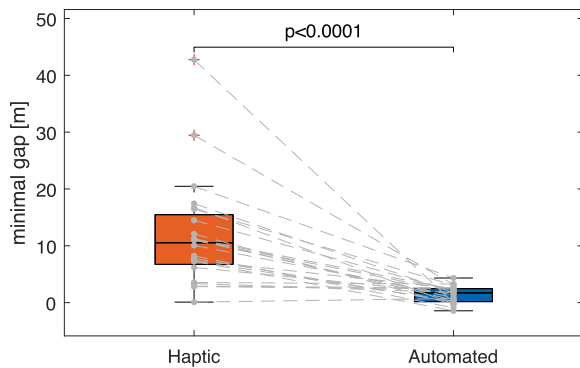


Fig. 16. Minimal bumper-to-bumper gap between the ego vehicle and the leading vehicle for the haptic and automated condition after the silent automation failure.

the gap reduces after the silent failure, but this reduction was never as drastic as in the automated case and values close to 0 were never reached (see Fig. 15). This is further illustrated by the minimal value the gap reached in 15 s after the failure (see Fig. 16). This minimal gap value was significantly larger in the haptic condition compared to the automated condition ( $t = 5.3917, p < 0.0001$ ). However, there was no evidence of a decrease in the number of collisions in the haptic condition compared to the automated condition (McNemar  $\chi^2 = 3.2, p = 0.073638$ ).

### E. User Acceptance

Subjective user acceptance of the haptic and fully automated controllers was measured using the Van der Laan questionnaire [36], which quantifies how the participants perceive a system in terms of usefulness and satisfaction. The questionnaire consists of nine questions where the participants grade the system on a five-point scale from  $-2$  to  $2$ .

Both haptic shared control and full automation were positively evaluated by the participants (see Fig. 17). Specifically, the means of the satisfaction and usefulness scores for both systems are significantly larger than zero, which means that the systems were rated as satisfactory (haptic  $t = 3.1855, p = 0.0041$ ,

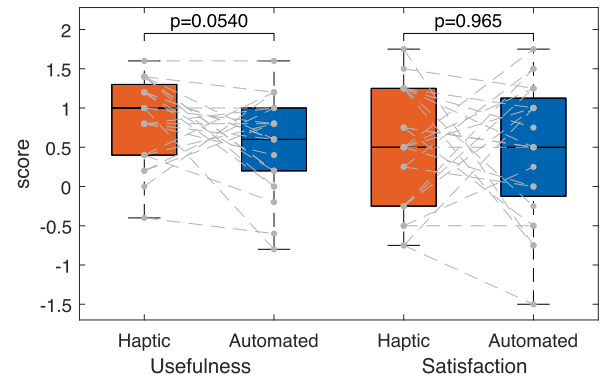


Fig. 17. Acceptance scores for the haptic shared control system and the automated system.

fully automated  $t = 2.7080, p = 0.0125$ ) and useful (haptic  $t = 8.0656, p < 0.0001$ , fully automated  $t = 4.5859, p = 0.0001$ ). We found no evidence of a difference in subjective usefulness ( $t = 2.030, p = 0.0541$ ) and user satisfaction ( $t = 0.044, p = 0.9650$ ) between the haptic shared control system and the fully automated system.

## V. DISCUSSION

Our results showed that haptic shared control reduced variability in vehicle motion and dissipated stop-and-go waves faster and more often than manual control. However, we found no evidence that haptic shared control resulted in improved road throughput. Full automation reduced variability in the ego vehicle behavior and improved traffic jam dissipation as well as vehicle throughput, compared to both manual control and haptic shared control. However, the fully automated system was less safe than haptic shared control in the event of the silent automation failure, as measured by the minimal gap to the leading vehicle. Both the haptic shared controller and the fully automated controller were rated positively by the users in terms of usefulness and satisfaction, and there was no evidence of a difference between the acceptance scores of the haptic and automatic systems. The fact that the achieved traffic jam dissipation performance of the haptic shared controller lies between the manual control case and the automated case is in line with our hypotheses. It is also in line with the essence of haptic shared control to blend manual control and automation.

The improved performance and reduced motion variability that the automation achieves over the manual control case are in line with the findings by Stern et al. [15], which evaluated a ring road scenario with the same circumference and amount of cars. Importantly, Stern et al. [15] managed to obtain much higher mean speeds (about 7.5 m/s) than our study (not higher than 4 m/s). This difference can be attributed to the fact that Stern et al. [15] instructed their participants to keep a much smaller time headway (gap/speed) than they would normally do while driving. To investigate whether this was the case, we extracted the mean distance gap over the whole platoon from the data of [15] and found it to be very similar to our study, both being around 7.8 m. The almost twofold difference in mean speed between our study and [15] given similar mean distance

gaps, therefore, indicates that drivers in [15] indeed kept much smaller time headways than in our study. We did not program the simulated human drivers in this study to keep a lower time headway, and neither did we instruct the human participants to do so because this is not in line with the driving behavior of regular human drivers. The comparatively low driving speeds in our experiment could, therefore, have led to a ceiling effect for the mean speed and throughput. This, in turn, could be the reason why we did not observe differences in these metrics between the manual case and the haptic shared control case.

Our findings are also in line with Jiang et al. [24], who evaluate a similar ring road scenario as [15], but with a shared algorithm instead of a fully automated algorithm. Their study shows that this sharing algorithm is able to stabilize traffic just like the automated controller from [15]. However, Jiang et al. [24] have not evaluated their controller in a human-in-the-loop experiment, only demonstrating it with simulated drivers. Their algorithm manages to stabilize traffic for every type of human driving behavior that was evaluated. We did not find this: some traffic jams were not solved for the haptic case. This difference can be explained either by discrepancies between the simulated and real humans or by the different controller type: we used a haptic shared controller, where the human can always fully overrule the automation. On the other hand, as mentioned in Section I, the nonhaptic shared control algorithm from [24] is designed in a way that the human driver only controls half of the inputs. While this leads to reduced speed variation, it could lead to reduced acceptance when driver and automation actions are misaligned, reduced safety margins, or even accidents in case of automation failures.

Our finding that the silent automation failure can result in decreased bumper-to-bumper gap and collisions in the automated case is in line with the previous findings about vigilance decrement and increased reaction times [17], [22]. This result, together with the finding that haptic shared control improves safety compared to full automation, also resonates with the study by Flemisch et al. [26], which evaluated a similar scenario for haptic shared control for lateral vehicle motion to illustrate the advantage of keeping the driver in the loop. Furthermore, four out of five participants that caused a collision experienced the automated case before the haptic case, which could imply that participants that already experienced the haptic automation failure were more alert for a failure.

The main limitations of the current study concern controller tuning and translating the finding to more realistic environments. First, the controller that calculates the target pedal position in the fully automated condition was tuned to have high gains, with the purpose of efficient dissipation of the traffic jam. However, high gains in some cases resulted in oscillatory behavior; even when there was no phantom traffic jam, the accelerator pedal moved relatively aggressively, as compared to the haptic and manual case [see Fig. 7(c)]. This behavior allowed the controller to keep the bumper-to-bumper gap close to the target value [see Fig. 5(c)] but is likely suboptimal in terms of perceived motion comfort and fuel consumption. We, therefore, recommend that future studies investigate how tuning the automation's controller gains can balance dissipating the traffic jams and minimizing acceleration/velocity oscillations.

Second, this study has only shown the efficacy of haptic shared control for an artificial ring road scenario at low speeds. Although this scenario shows the promise of haptic shared control, it does not generalize to real-world scenarios in several ways. First, phantom traffic jams occur on highways where cars drive at speeds in the range of 80–120 km/h. In this scenario, velocities range from 0 to 20 km/h. The ring road itself is also not representative of actual highways, which are usually straight and multilane. Furthermore, in a multilane scenario, the operation of longitudinal driving automation could be affected by lateral driving automation (e.g., lane-keep assist). Finally, our implementation of the silent automation failure is much simplified. For these reasons, an important direction for future research is evaluating our controller in more realistic scenarios, studying the effects of higher speeds, lateral automation, and more realistic automation failures.

## VI. CONCLUSION

This article proposed a haptic shared control system designed to dissipate phantom traffic jams. We evaluated the system against manual control and full automation in a human-in-the-loop driving simulator experiment. We conclude that:

- 1) haptic shared control dissipates phantom traffic jams faster and more often compared with manual control;
- 2) full automation dissipates traffic jam faster than haptic shared control but leads to increased occurrence of unsafe situations in case of a silent automation failure.

We concluded that haptic shared control shows promise for mitigating phantom traffic jams while preventing safety risks associated with full driving automation.

## ACKNOWLEDGMENT

The authors would like to thank Cruden driving simulators B.V. for facilitating hardware, software, and knowledge, all of which were necessary for building the setup used in this study.

## REFERENCES

- [1] K. Mahmud, K. Gope, and S. M. R. Chowdhury, "Possible causes & solutions of traffic jam and their impact on the economy of Dhaka city," *J. Manage. Sustain.*, vol. 2, 2012, Art. no. 112.
- [2] F. Wu et al., "Tracking vehicle trajectories and fuel rates in phantom traffic jams: Methodology and data," *Transp. Res. C, Emerg. Technol.*, vol. 99, pp. 82–109, 2019.
- [3] K. Goldmann and G. Sieg, "Economic implications of phantom traffic jams: Evidence from traffic experiments?" *Transp. Lett.*, vol. 12, no. 6, pp. 386–390, 2020.
- [4] M. Treiber and A. Kesting, "Traffic flow dynamics," in *Traffic Flow Dynamics: Data, Models and Simulation*. Berlin, Germany: Springer, 2013.
- [5] B. S. Kerner, *The Physics of Traffic* (Understanding Complex Systems Series), J. A. S. Kelso, Ed. Berlin, Germany: Springer, 2004.
- [6] R. Kühne, R. Mahnke, I. Lubashevsky, and J. Kaupužs, "Probabilistic description of traffic breakdowns," *Phys. Rev. E*, vol. 65, no. 6, 2002, Art. no. 066125.
- [7] R. J. M. Kaupužs and I. Lubashevsky, "Probabilistic description of traffic flow," *Phys. Rep.*, vol. 408, no. 1/2, pp. 1–130, Mar. 2005.
- [8] J. Lee and J. H. Kim, "Phantom traffic: Platoon formed at low traffic density," *J. Transp. Eng. A, Syst.*, vol. 145, no. 2, 2019, Art. no. 04018082.
- [9] Y. Sugiyama et al., "Traffic jams without bottlenecks—Experimental evidence for the physical mechanism of the formation of a jam," *New J. Phys.*, vol. 10, no. 3, 2008, Art. no. 033001.
- [10] S.-i. Tadaki et al., "Phase transition in traffic jam experiment on a circuit," *New J. Phys.*, vol. 15, no. 10, 2013, Art. no. 103034.

- [11] G. Gunter et al., "Are commercially implemented adaptive cruise control systems string stable?," *IEEE Trans. Intell. Transp. Syst.*, vol. 22, no. 11, pp. 6992–7003, Nov. 2021.
- [12] S. Hoogendoorn, W. Daamen, R. Hoogendoorn, and J. Goemans, "Assessment of dynamic speed limits on Freeway A20 near Rotterdam, Netherlands," *Transp. Res. Rec.*, vol. 2380, no. 1, pp. 61–71, 2013.
- [13] J. Kim, J. Jeong, K.-y. Jhang, and J.-h. Park, "Demonstration of disturbance propagation and amplification in car-following situation for enhancement of vehicle platoon system," in *Proc. IEEE Intell. Veh. Symp.*, 2015, pp. 999–1005.
- [14] A. R. Kreidieh, C. Wu, and A. M. Bayen, "Dissipating stop-and-go waves in closed and open networks via deep reinforcement learning," in *Proc. 21st Int. Conf. Intell. Transp. Syst.*, 2018, pp. 1475–1480.
- [15] R. E. Stern et al., "Dissipation of stop-and-go waves via control of autonomous vehicles: Field experiments," *Transp. Res. C, Emerg. Technol.*, vol. 89, pp. 205–221, 2018.
- [16] M. Čičić and K. H. Johansson, "Traffic regulation via individually controlled automated vehicles: A cell transmission model approach," in *Proc. 21st Int. Conf. Intell. Transp. Syst.*, 2018, pp. 766–771.
- [17] R. Parasuraman, "Human-computer monitoring," *Hum. Factors*, vol. 29, no. 6, pp. 695–706, 1987.
- [18] L. Bainbridge, "Ironies of automation," in *Analysis, Design and Evaluation of Man-Machine Systems*. Amsterdam, The Netherlands: Elsevier, 1983, pp. 129–135.
- [19] D. R. Davies and R. Parasuraman, *The Psychology of Vigilance*. Orlando, FL, USA: Academic, 1982.
- [20] B. Son, T. Kim, and Y. Shin, "A solution for the dropout problem in adaptive cruise control range sensors," in *Proc. Int. Conf. Embedded Ubiquitous Comput.*, 2006, pp. 979–987.
- [21] L. Nilsson, *Safety Effects of Adaptive Cruise Controls in Critical Traffic Situations*. Linköping, Sweden: Statens väg-och transportforskningsinstitut, 1996.
- [22] C. M. Rudin-Brown and H. A. Parker, "Behavioural adaptation to adaptive cruise control (ACC): Implications for preventive strategies," *Transp. Res. F, Traffic Psychol. Behav.*, vol. 7, no. 2, pp. 59–76, 2004.
- [23] P. A. Hancock, "Some pitfalls in the promises of automated and autonomous vehicles," *Ergonomics*, vol. 62, no. 4, pp. 479–495, 2019.
- [24] J. Jiang, A. Astolfi, and T. Parisini, "Robust traffic wave damping via shared control," *Transp. Res. C, Emerg. Technol.*, vol. 128, 2021, Art. no. 103110.
- [25] D. A. Abbink and M. Mulder, "Neuromuscular analysis as a guideline in designing shared control," in *Advances in Haptics*, M. H. Zadeh, ed. Rijeka, Croatia: InTech, 2010, pp. 499–516.
- [26] F. Flemisch, J. Kelsch, C. Löper, A. Schieben, J. Schindler, and M. Heesen, "Cooperative control and active interfaces for vehicle assistance and automation," in *Proc. FISITA World Automot. Congr.*, 2008, p. F2008-02-045.
- [27] M. Mulder, M. Mulder, M. Van Paassen, and D. Abbink, "Haptic gas pedal feedback," *Ergonomics*, vol. 51, no. 11, pp. 1710–1720, 2008.
- [28] E. Adell, A. Várhelyi, and M. Hjälm Dahl, "Auditory and haptic systems for in-car speed management—A comparative real life study," *Transp. Res. F, Traffic Psychol. Behav.*, vol. 11, no. 6, pp. 445–458, 2008.
- [29] S. Azzi, G. Reymond, F. Mérienne, and A. Kemeny, "Eco-driving performance assessment with in-car visual and haptic feedback assistance," *J. Comput. Inf. Sci. Eng.*, vol. 11, no. 4, 2011, Art. no. 041005.
- [30] A. Jamson, D. L. Hibberd, and N. Merat, "The design of haptic gas pedal feedback to support eco-driving," in *Proc. 7th Int. Driving Symp. Hum. Factors Driver Assessment, Training, Veh. Des.* 2013, pp. 264–270.
- [31] J. Zhao, G. Shen, C. Yang, G. Liu, L. Yin, and J. Han, "Feel force control incorporating velocity feedforward and inverse model observer for control loading system of flight simulator," *Proc. Inst. Mech. Eng. I, J. Syst. Control Eng.*, vol. 227, no. 2, pp. 161–175, 2013.
- [32] M. Mulder, D. A. Abbink, M. M. Van Paassen, and M. Mulder, "Design of a haptic gas pedal for active car-following support," *IEEE Trans. Intell. Transp. Syst.*, vol. 12, no. 1, pp. 268–279, Mar. 2010.
- [33] R. Van Gaal, "Panthera software," 2022. [Online]. Available: <https://www.cruden.com/panthera-software/>
- [34] I. A. Group, "IPG carmaker reference manual version 9.1," 2020. [Online]. Available: <https://www.ipg-automotive.com/>
- [35] Q. McNemar, "Note on the sampling error of the difference between correlated proportions or percentages," *Psychometrika*, vol. 12, no. 2, pp. 153–157, 1947.
- [36] J. D. Van Der Laan, A. Heino, and D. De Waard, "A simple procedure for the assessment of acceptance of advanced transport telematics," *Transp. Res. C, Emerg. Technol.*, vol. 5, no. 1, pp. 1–10, 1997.